Int. J. Solids Structures, 1975, vol. 11, pp. 75–87. Pergamon Press. Printed in Gt. Britain.

ON THE BEHAVIOR OF STRESS WAVES IN COMPOSITE MATERIALS—II. THEORETICAL AND EXPERIMENTAL STUDIES ON THE EFFECTS OF CONSTITUENT DEBONDING†

D. S. DRUMHELLER and C. D. LUNDERGAN

Members of Technical Staff Sandia Laboratories, Albuquerque, New Mexico 87115, U.S.A.

(*Received* 13 *December* 1973)

Abstract—The theory derived in Part I is compared to data obtained from flyer-plate experiments on laminated composites. The composites were constructed of alternating layers of aluminum and polymethyl methacrylate. Impact occurred on a flat plane oriented perpendicular to the interface planes of the composite constituents. As opposed to the behavior of a fully bonded composite which allows only one longitudinal stress wave to propagate through its interior, two longitudinal stress waves were observed in the debonded composite.

Reasonable agreement was achieved in the comparisons of theory to experiment after adjustment was made for the effect of residual bond strength at the constituent interfaces.

INTRODUCTION

A theoretical basis for describing the effects of constituent debonding was derived in Part I of this paper. The central element of the derivation is embodied in the concept that when the bonds between the constituents deteriorate, an additional degree of freedom is achieved within the composite, and that under dynamic loading conditions this results in an additional stable propagating stress wave.

It now remains to compare the results of this theory to data obtained from controlled experiments on model composites. As is always appropriate, the experiments have been optimized to minimize the effects of extraneous behavior. The specimens are constructed of laminae to facilitate a direct comparison to the theory. Also, on the average, induced deformations are limited to one-dimensional strain, and the resulting stress levels, while high enough to produce debonding between the laminae, are low enough to result in an approximately linear material response.

In the sequel the experiments will be described along with a discussion as to their accuracy and repeatability. Then the experimental data will be compared to the results of the theory derived in Part I. The additional complication of residual bond strength will also be discussed.

EXPERIMENTAL PROCEDURE

Since in many cases commercial composite materials are susceptible to a wide variety of extraneous responses due to the effects of nonuniformity, porosity, etc. a set of laminated composite specimens were constructed using highly controlled fabrication techniques.

† This work was supported by the United States Atomic Energy Commission.

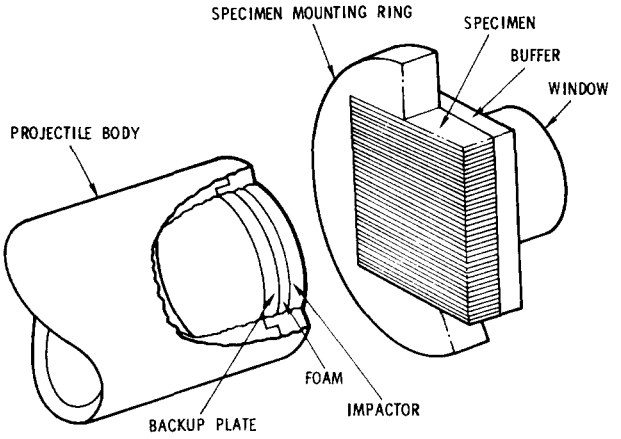

Fig. 1. The experimental configuration.

Each composite was constructed from plates of polymethyl methacrylate (PMMA, Rohm and Haas Type A) 0·762-mm thick and plates of 6061-T6 aluminum 0·792-mm thick. By following the procedures outlined in Reference[1], the plates or laminae were bonded together to form a periodic structure with 48 unit cells each composed of an aluminum and a PMMA laminae with bond strengths on the order of 0·2 kbar.

In each experimental configuration, Fig. 1 and Table 1, the laminae of the composite were oriented perpendicular to the impact plane and struck by a flat-faced projectile fired from a 10-cm bore light gas gun[2]. In this type of experiment, absolute time references are normally established at the moment of impact; but to accomplish this requires extremely flat impact surfaces on both the projectile and the specimen. The flatness is usually measured with an optical flat; however, the nature of the composite surface which contained striped areas of both aluminum and PMMA prevented an accurate determination of flatness. Consequently, an accurate time base could not be established. While there was no absolute time base, the relative time scale, i.e. the distance between any two points on the time scale, was determined to within 0·002 μsec.

Table 1. The experimental configurations†

Experiment No.	Composite thickness (cm)	Projectile		
		Material	Velocity (cm/μsec)	Thickness (cm)
1	0·820	aluminum	0·001355	1·634
2	0·776	aluminum	0·001420	1·631
3	0·806	aluminum	0·001144	1·571
4	0·803	PMMA	0·002118	0·691
5	0·805	PMMA	0·003078	0·694
6	0·812	tungsten carbide	0·001289	0·975
7	0·810	aluminum	0·001330	0·656
8	0·809	aluminum	0·001066	0·164

† In all experiments the buffer plate was 1 cm thick. The bond thicknesses were all less than 0·0002 cm thick.

Following impact the ensuing stress waves traveled through the specimen and into a 6061-T6 aluminum buffer plate. This plate was used to improve the coherence of the transmitted wave front. The wave then traveled into the transparent Dynasil 1000 window material. A small thin mirror was vapor deposited on the window at the buffer-window interface, and the motion of this mirror was measured to within $\pm 1{\cdot}5 \times 10^{-5}$ mm with a displacement interferometer[3]. The data collection was completed before release waves from either the lateral surfaces of the projectile, specimen, buffer, and window or the rear surface of the window could reach the mirror. Thus an average condition of one-dimensional strain existed during this time.

The accuracy of the data was also affected by tilting of the projectile prior to impact. While this tilting is normally less than 0·03 degrees, it could not be measured directly because of the problem associated with the specimen flatness. However, as shown in[1], the effects of excessive tilt are indirectly manifested in a periodic pinching of the amplitude of the interferometer data traces. In this set of experiments only the data traces from Experiment 1 exhibited pinching. Experiment 1 was repeated in Experiment 3, and, like the remaining data traces, Experiment 3 did not exhibit pinching. The results of these two experiments are compared in Fig. 2 which is a plot of particle velocity of the mirror versus relative time. The pronounced differences result from the low tilt in Experiment 3 and the high tilt in Experiment 1. Unless, as in Experiments 2–8, the tilt is kept small, the data are generally useless.

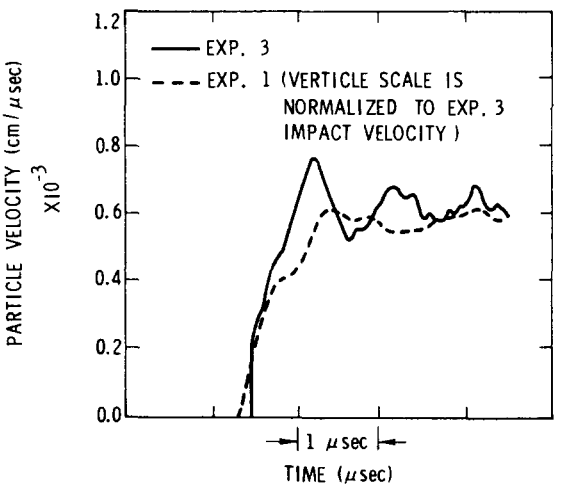

Fig. 2. The effect of excessive projectile tilt.

In addition to having little tilt these experiments have a high degree of reproducibility. For example, the results of Experiments 4 and 5 which are similar, except for the impact velocities, have been normalized to a common impact velocity and compared in Fig. 3. Except for Experiment 1, the degree of reproducibility shown in Fig. 3, which results in part through the use of a relatively thick buffer plate to "smooth" the waves, has been attained in all the experiments.

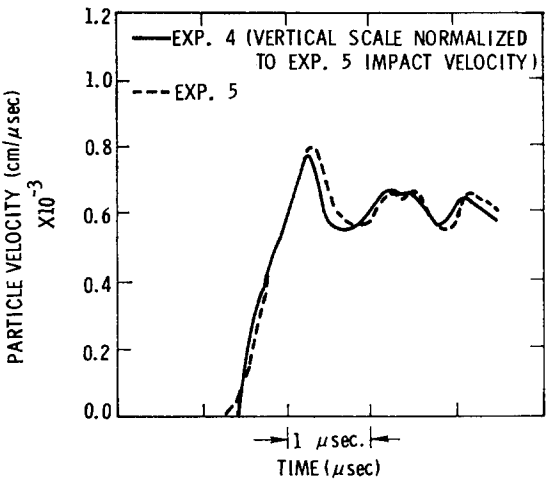

Fig. 3. The repeatability of the flyer-plate experiment.

ANALYSIS

The most direct way to introduce this section is to first qualitatively compare data from one of the experiments to what shall be called the standard wave profile. The standard wave profile, i.e. one that is free of debonding effects, is usually observed either when the composite is shock loaded with a low pressure pulse or when high pressure shock pulses propagate perpendicular to the reinforcing direction. In both these cases debonding is absent. Figure 4 contains an example of this type of profile. A single longitudinal wave is generated which has a long even rise at the wavefront followed by a ringing motion with a single dominant frequency.

In contrast, the solid line in Fig. 5 shows the results of Experiment 2. Because the waves propagated along the laminae of the composite, no propagating shear wave was generated; however, two distinct longitudinal waves are present and the ringing behind the wavefronts

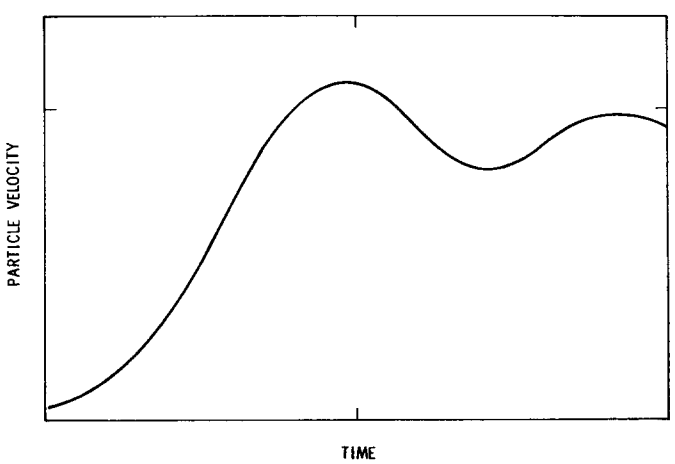

Fig. 4. The standard wave profile.

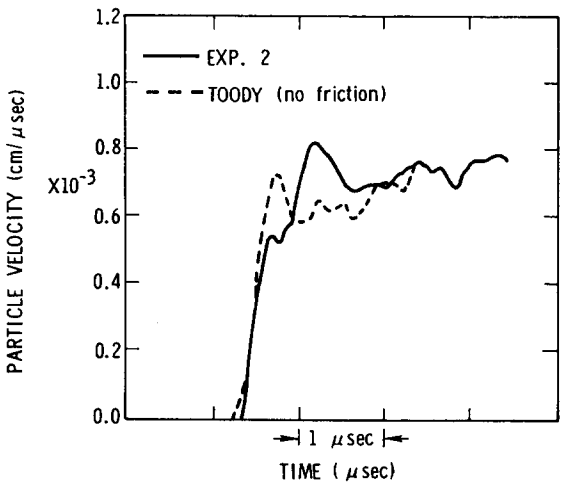

Fig. 5. Comparison of Experiment 2 to TOODY without friction.

has several dominant frequencies. In this case, the effects of debonding are quite pronounced and the use of conventional models, which are based on the assumption of perfect bonding, will prove to be inadequate.

In a similar manner the assumption of total debonding may also prove to be unsatisfactory. Consequently, as a preliminary to presenting the comparisons between Part I and the experimental data, the subject of residual bond strength will be discussed. For calculational convenience it will be treated as a frictional force which exists at the interfaces of the laminae uniformly throughout the composite.

Table 2. Material properties

Material	Lamé constants (kbar) λ	μ	Density (g/cm³)
PMMA	41·2	22·9	1·2
aluminum	569	272	2·7
tungsten carbide	2074	2980	14·85
Dynasil 1000 (fused quartz)	147·4	313	2·201

To study this effect a two-dimensional Lagrangian wave propagation code, TOODY-II, was used to model Experiment 2[4]. This code is based on the finite-differenced form of the equations of mass, momentum, and energy conservation from continuum mechanics. Because of the low experimental stress levels, all of the materials were treated as linearly elastic according to the properties listed in Table 2. Because of the symmetry conditions, only the region bounded by center planes of two adjacent laminae were modeled in the

code.† Sliding was allowed between the two laminae, and the frictional force was proportional to the local normal stress pushing the two laminae together.

Several TOODY calculations were made using different coefficients of friction. Two of these calculations are compared to the data of Experiment 2 in Figs. 5 and 6. Figure 5 contains the results for zero friction or total debonding, and Fig. 6 contains the results for coefficient of friction of 1·8 or partial debonding. Comparison of these two figures reveals a rather pronounced difference. For zero friction in the TOODY calculation, the second wave lags the lead wave by almost two microseconds and is hardly recognizable as a separate wave. In contrast the calculation which includes friction shows a faster traveling second wave with a more dominant profile. This calculation is in good agreement with the experimental data. Of course if the frictional coefficient were increased even further, the two calculated waves would eventually merge to a single wave profile similar to that of the standard wave profile.

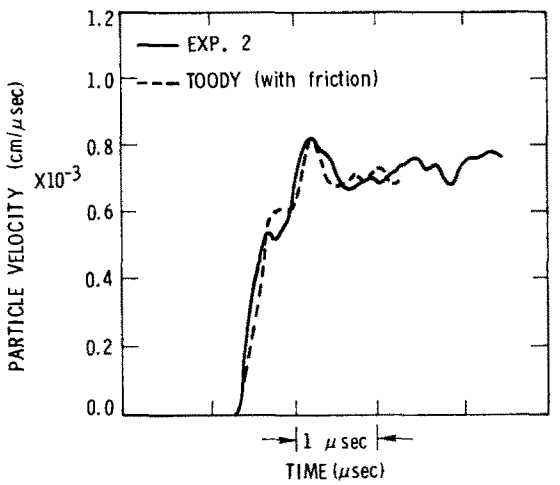

Fig. 6. Comparison of Experiment 2 to TOODY with friction.

From the preceding arguments, it can be concluded that the effects of residual bond strength play an important role in the overall response of the composite. Consequently, any meaningful comparisons between the experimental data and the results of the theory in Part I must include this effect in the calculations. Unfortunately, at present there is no rigorous procedure for incorporating this effect directly into the field equations shown in Appendix B of Part I. Instead, indirect compensation will be made by arbitrarily increasing the calculated propagation velocity of the second wave.

If the properties listed in Tables 1 and 2 are substituted into the relations derived in Part I, propagation velocities of 0·560 cm/μsec for the first wave and 0·266 cm/μsec for the second wave are obtained. The results of this calculation are compared to the frictionless TOODY calculations in Fig. 7.‡ Considering that geometric wave dispersion is not included in the

† For reference, 17 finite-difference zones were used across the thickness of the laminae contained between the symmetry planes.

‡ The derivation of Part I ignored the buffer–window interface; however, the effect of this interface was included by increasing the calculated particle velocities by seven per cent.

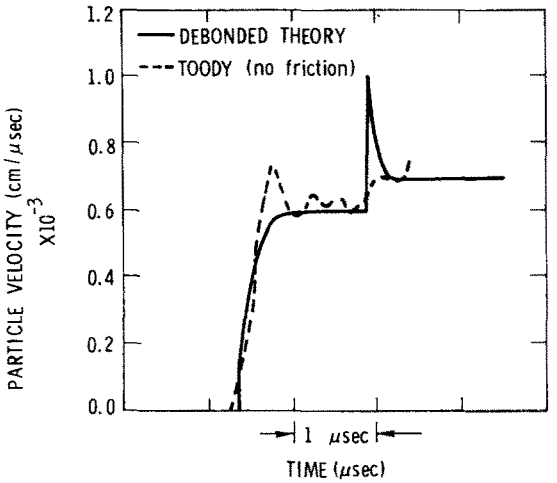

Fig. 7. Comparison of debonded theory to TOODY without friction.

results from Part I, the agreement with TOODY is quite good; especially for the wave velocities. When the calculation for the propagation velocity of the second wave is increased to 0·344 cm/μsec and then compared to the TOODY calculation with friction, the comparison in Fig. 8 is obtained.

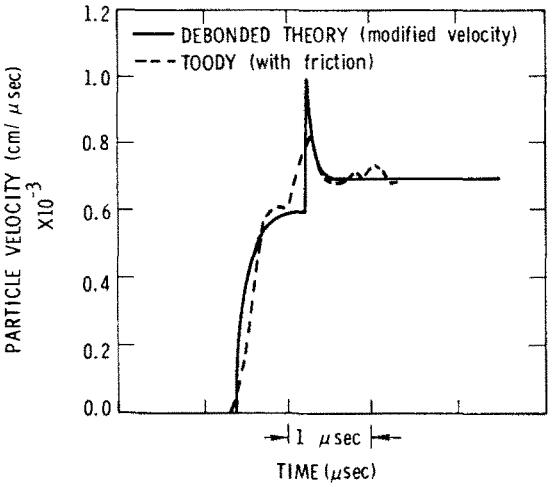

Fig. 8. Comparison of debonded theory with modified velocity to TOODY with friction.

In the sequel, the calculations based on Part I will include results using both the low and high velocities for the second wave to illustrate the effects of both total and partial debonding.

RESULTS

The results from Part I using both the original velocities and modified velocities are compared to Experiments 2 through 8 in Figs. 9–15. These comparisons include PMMA, aluminum, and tungsten carbide impactors, and both step-function and square-pulse input

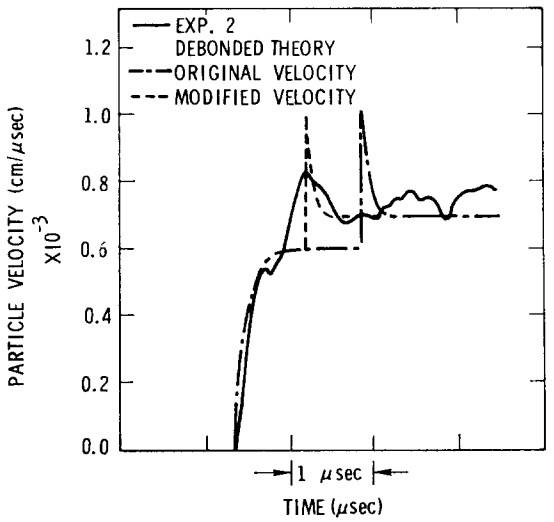

Fig. 9. Comparison of debonded theory to Experiment 2.

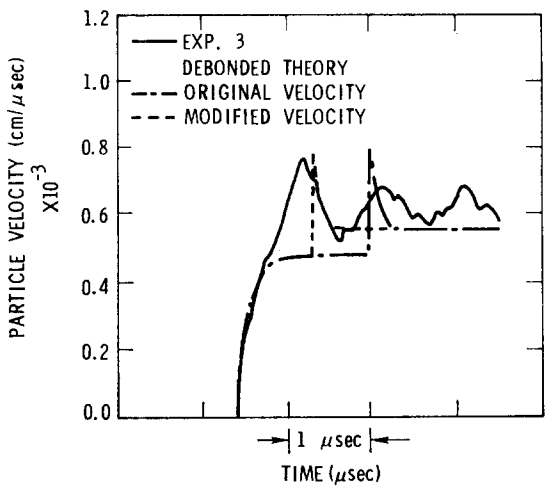

Fig. 10. Comparison of debonded theory to Experiment 3.

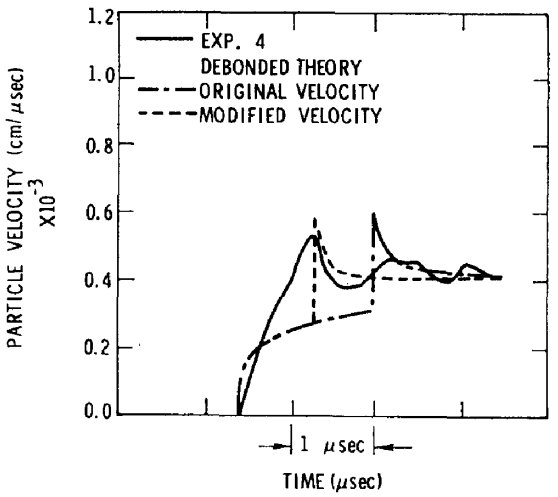

Fig. 11. Comparison of debonded theory to Experiment 4.

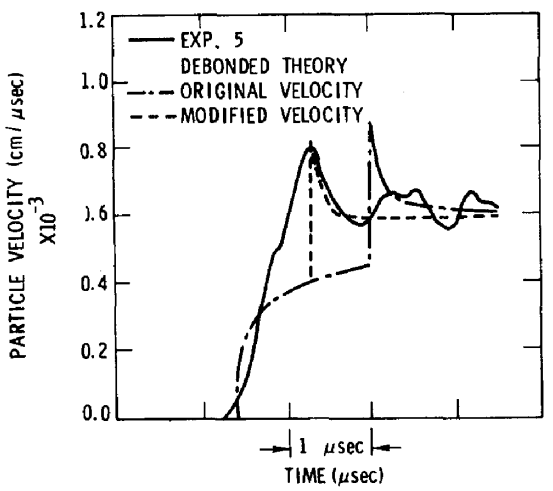

Fig. 12. Comparison of debonded theory to Experiment 5.

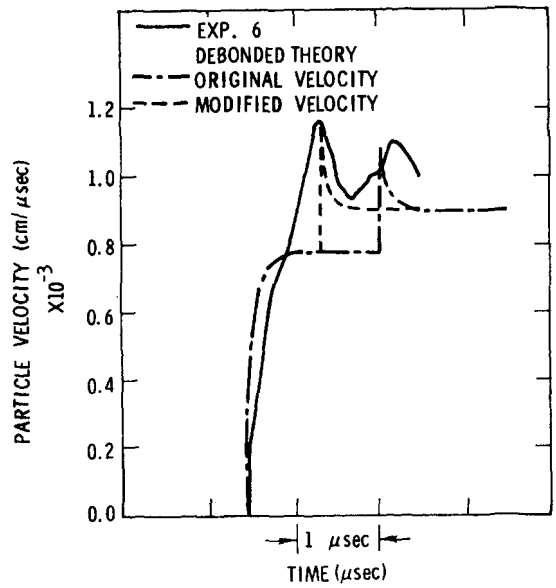

Fig. 13. Comparison of debonded theory to Experiment 6.

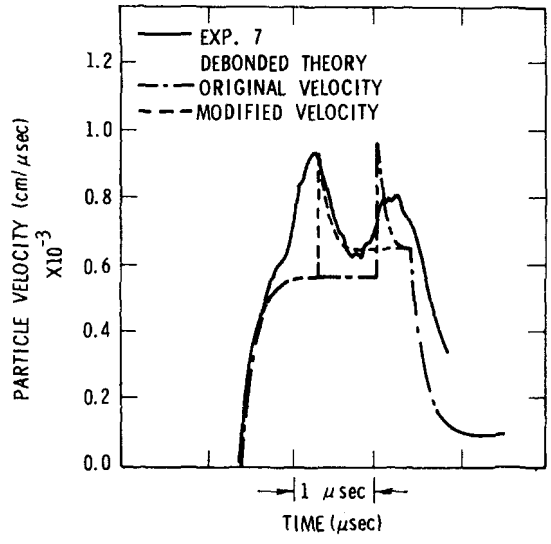

Fig. 14. Comparison of debonded theory to Experiment 7.

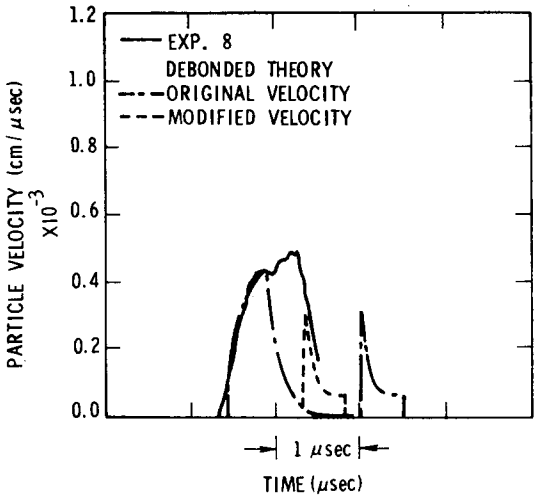

Fig. 15. Comparison of debonded theory to Experiment 8.

waves. Considering the discrepancy due to lack of wave dispersion in the calculation, the comparisons for the lead wave are good. The comparisons for the second wave, while less accurate, are still encouraging. Geometric dispersion once included in the calculations would attenuate most of the spiked profile associated with the calculation for the second wave. In all cases the omission of the effects of residual bond strength produces serious errors in the calculated results.

Along with the particle-velocity profiles, three stress profiles have been included in Figs. 16–18. These plots represent the normal stress in the direction of propagation in both the PMMA and aluminum laminae for Experiments 5, 2 and 6 using PMMA, aluminum, and tungsten carbide impactors, and show that the lead wave travels mainly in the aluminum, and the second wave travels mainly in the PMMA.

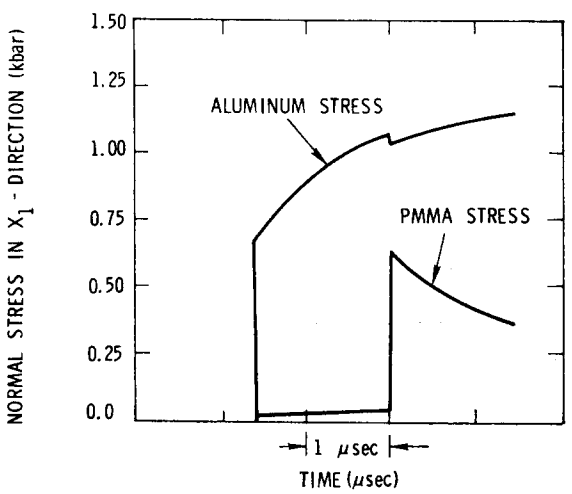

Fig. 16. Normal stress in composite for PMMA projectile, Experiment 5.

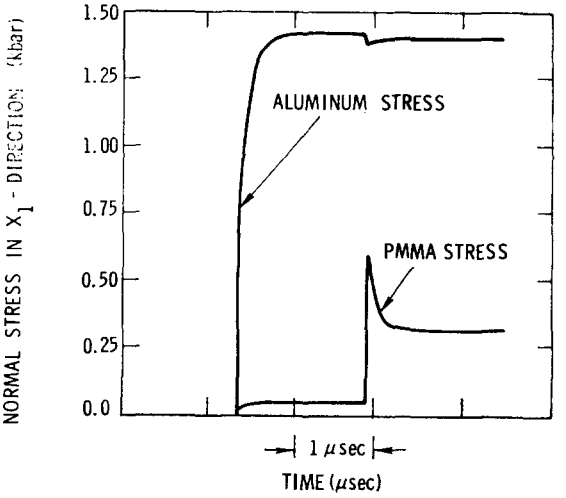

Fig. 17. Normal stress in composite for aluminum projectile, Experiment 2.

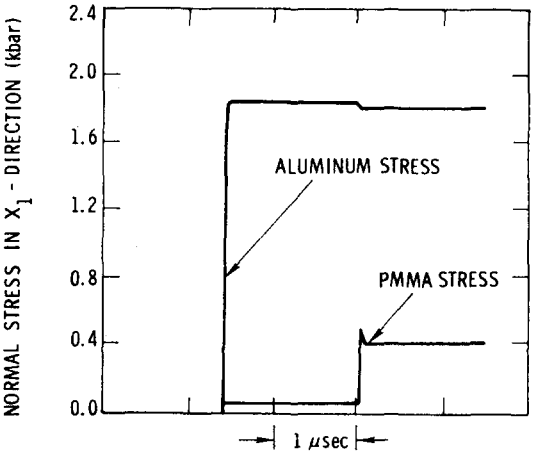

Fig. 18. Normal stress in composite for tungsten carbide projectile, Experiment 6.

The previous calculations and experimental data can also be compared to a conventional theory based on bonded constituents. This is the equivalent modulus theory of Postma which also neglects geometric wave dispersion and predicts the arrival of a single longitudinal stress wave[5]. For the semi-infinite pulse experiment, it predicts a step pulse propagating at 0·502 cm/μsec with an amplitude equal to the final amplitude predicted by the debonded calculations. For Experiments 7 and 8, the Postma theory predicts single square pulses, 2 μsec and 0·5 μsec wide respectively. These wave velocities place the Postma wavefront approx 0·16 μsec behind the leading wavefront of the debonded calculations.†

It is interesting to note that both theories predict the same final amplitude for the semi-infinite waves. This is explained through the observation that the debonded calculations

† Because of the simple wave forms associated with the Postma results and for clarity in the illustrations, these results have not been included in the figures.

predict equal final velocities for both composite constitutents. Obviously the bonded theory predicts the same result.

While the effects of geometric wave dispersion are not included in the calculations, the qualitative nature of this phenomena can still be discussed. For the bonded theory dispersion tends to filter the high frequency components of the stress wave causing it to be altered from a step pulse to a wave with a finite rise time followed by a ringing motion[6]. The ringing motion has one dominant frequency related directly to the internal geometry of the composite and the propagation velocity of the disturbance. It seems logical that two waves with different propagation velocities would each have different ringing frequencies. The combined effect would be the complex ringing pattern observed in the experimental data

CONCLUSIONS

This work has illustrated the important role that debonding plays in the dynamic response of composite materials. Both analytical and experimental techniques have been used to establish the existence and to study the behavior of an additional mode of wave propagation. Although the theory of Part I accounts for only the most basic mechanisms of the problem, the agreement with experiment is still reasonably good. Extension of this theory will require a rigorous procedure for the inclusion of the effects of residual bond strength. The residual bond strength of the composite causes the lagging longitudinal wave to travel faster but has no influence on the final particle velocity of the material.

While the theory presented in Part I is not the ultimate answer to modeling debonded composites, it does contain a number of fundamental concepts necessary for achieving this goal: the theory allows for the existence of an additional propagation mode; the concept of warping at the composite boundary is a logical and necessary inclusion to provide for compatibility between the boundary conditions and the field equations; and the theory, when appropriate, reduces to the conventional system used for fully bonded composites.

REFERENCES

1. C. D. Lundergan and D. S. Drumheller, The Propagation of Transient Pulses in an Obliquely Laminated Composite, *Dynamics of Composite Materials*, edited by E. H. Lee. American Society of Mechanical Engineers (1972).
2. L. M. Barker and R. E. Hollenbach, Systems for Measuring the Dynamic Properties of Materials, *Rev. Sci. Instruments*, **35**, 742–746 (1964).
3. L. M. Barker and R. E. Hollenbach, Interferometer Technique for Measuring the Dynamic Properties of Materials *Rev. Sci. Instruments*, **36**, 1617–1620 (1965).
4. L. D. Bertholf and C. H. Karnes, Axisymmetric Elastic–Plastic Wave Propagation in 6061-T6 Aluminum Bars of Finite Length, *J. Appl. Mech.* **36**, 533–541 (1969).
5. G. W. Postma, Wave Propagation in a Stratified Medium, *Geophysics*, **20**, 780–806 (1955).
6. D. S. Drumheller and H. J. Sutherland, A Lattice Model for Stress Wave Propagation in Composite Materials, *J. Appl. Mech.* **40**, 149–154 (1973).

Абстракт — Теория, выведена в части 1 сравнивается с данными, полученными из экспериментов плиток маховиков, изготовленных из слоистых материалов. Эти слоистые материалы построены из переменных слоев алюминия и полиметилметакрилата. Удар происходит по плоской поверхности, которая ориентирована перпендикулярно к плоскостям раздела компонентов слоистых материалов. В противоположности к поведению полно соединенных слоистых материалов, которые дают возможность распространения одной продольной волны напряжения сквозь их внутренную область, в разъединенных слоистых материалах наблюдаются две продольные волны напряжения.

Получается умеренное согласие теории в сравнении с экспериментом, после корректировки эффекта сопротивления остаточной связи на поверхностях раздела компонентов.